COBEM 2023 27TH INTERNATIONAL CONGRESS OF MECHANICAL ENGENEERING

ABCM Brazilian Society of Mechanical Sciences and Engineering
27th ABCM International Congress of Mechanical Engineering
December 04-08, 2023, Florianópolis-SC, Brazil

COB-2023-XXXX
THE USE OF THERMOGRAPHY IN THE DETECTION OF BREAKAGE IN STEEL: FAILURE PREVENTION IN THE TENSION PROCESS

Carlos Alberto Vicari
Universidade Federal do Paraná
carlos.vicari@ufpr.br

Maria Lucia Leite Ribeiro Okimoto
Universidade Federal do Paraná
lucia.demec@ufpr.br

Pablo Deivid Valle
Universidade Federal do Paraná
pablo.valle@ufpr.br

Bruno Ferrari de Almeida Prado
Universidade Federal do Paraná
brunoprado@ufpr.br

Samuel Cavalli Kluthcovsky
Universidade Federal do Paraná
samuelkluthcovsky@ufpr.br

Paulo Victor Prestes Marcondes
Universidade Federal do Paraná)
marcondes@ufpr.br

Abstract. *Thermography is being used more and more and in several areas. With the introduction of infrared cameras with better features and more affordable prices, it shows a possibility of using this technology to verify the behavior of the temperature in tensile strength test in steels. Thus, this work presents a validation of the use of infrared thermography in the study of the behavior of metallic sheets subjected to tensile stress. The process consists of carrying out tensile tests on BH 220 steel specimens and measure the tension and temperature up to the specimen's breaking point. At the end, it will be possible to verify if it is possible to evolve in this research field.*

Keywords: *Thermography, Steel BH220, Tensile test, Temperature, Infrared.*

1. INTRODUCTION

Several manufacturing industries use steel forming to produce parts and products and the automotive industry is at the forefront in its use of developing more efficient processes and materials. Bhattacharya (2014) explains that the search for weight reduction and compliance with the reduction of the environmental impact in the production of vehicles made the automotive industry start the search for new materials that meet these requirements. With this, the study of advanced high strength steels as well as their production methods and assembly techniques are becoming one of the main objectives of this sector according to Andrade et al (2002).

In this sense, according to Ferreira et al (2013), the use of steels such as BH220 in automotive panels aims to reduce the thickness of the plates, thus reducing their weight and consequently reducing fuel consumption.

Knowing the behavior of these steels and finding processes to minimize problems in forming parts is extremely important for the industry, especially the automobile industry. For Tekkaya at al (2020) failures in the forming process directly influence the cost of producing parts as well as reducing the reliability of parts produced and delivered to customers.

In this way, identifying methods to minimize or avoid production failures must always be analyzed and research in this direction aims to bring new ways to improve. In a review of the bibliography, it was possible to verify the use of thermographic analysis for detecting failures in already formed sheets, but in these cases the failure has already occurred and there is loss of the produced part, which causes waste. Therefore, this study aims to find out if it is possible to use thermographic analysis to predict failure before it occurs.

This study aims to perform tensile tests on specimens of BH220 steel, in order to study its thermal behavior during the test and identify significant and predictable variations that could lead to the rupture of the tested material.

In this study, the specimens will be subjected to tensile stress and, through a thermal camera, the temperature values will be analyzed from the initial time to the moment of rupture. This analysis will allow the understanding of the thermal behavior of the specimens during the tensile test and the identification of significant variations that may be associated with the occurrence of rupture.

2. LITERATURE REVIEW

Infrared thermography is a technique that uses thermographic cameras to measure and record the infrared radiation emitted by objects. This radiation is converted into thermal images that represent the temperature distribution of a given surface. According to Silva et al. (2019) infrared thermography appears in 1800 when scientist William Herchel accidentally discovers this principle, progressively spreading to various applications.

For years, infrared thermography techniques were improved and applied in various sectors, but it was during the Second World War that the use of thermography showed its value, mainly in capturing images in night actions (Lucchi, 2018).

2.1 USE OF THERMOGRAPHY IN METAL FAULT DETECTION

In industrial applications, it is common to design mechanical components with different shapes and details, such as holes, bumps, grooves, among others, to meet specific functional requirements. According to Shun-Peng at al(2022), these geometric details can result in stress concentrations, leading to complex stress-strain states and, in some cases, even localized plastic deformations. It is also emphasized in Shun-Peng at al(2022) that most fatigue failures in metallic parts occur in regions close to the root of the notch, where stress distributions become particularly complex.

The study of the behavior of cracked metals, subjected to dynamic loads, implies knowledge of both the stress intensity factor and the crack growth rate (Ancona, 2016). These parameters are, in general, obtained through conventional methods according to the standards ASTM E466 and ASTM E606/E606M and through non-destructive experimental techniques. The most widespread methods to monitor and measure the growth rate of cracks are microscopy analysis, extensometry, ultrasound, X-rays and DIC-“Digital Image Correlation” .(Ancona et al., 2016).

Currently, the detection of defects and internal and superficial flaws is used, normally using Non-Destructive Tests (NDT), among which visual inspection, magnetic particles, ultrasound, radiography, penetrating liquids and eddy currents. (Martína, 2015).

In Mohameda et al..(2019) it is seen that automatic crack detection helps to reduce costs and improve quality in surface inspection.

2.2 PASSIVE AND ACTIVE THERMOGRAPHY

There are two basic configurations for the implementation of an infrared thermography which are passive and active. In passive thermography, the monitoring of thermal radiation, emitted by the surface of the specimen under natural conditions, is used and is widely applied as a standard quality control technique of structures with historic value since many years ago (An et al 2012).

Among the different NDT techniques, thermal imaging helps to accurately obtain information on underground characteristics without compromising the structural integrity of the inspected target (An et al 2012). In addition, the use of thermography for an NDT analysis guarantees the possibility of not needing physical contact with the target.

The active configuration is implemented by generating a flow of heat such that the thermophysical properties of the test object can be made to enhance or impede this flow (An et al 2012).

The NDT procedures nowadays is typically based on active thermography because of its many advantages, such as more reliable information on its results and insensitivity to the influence of environments, An et al (2012). Figure 1 shows a typical classification of common infrared thermography methods. For An et al (2012), among all these active thermography techniques, pulsed phase thermography (PPT) and lock-in thermography (LIT) are the most applied. Thus, the methods of detecting defects in sheet metal parts were focused on the PPT and LIT techniques.

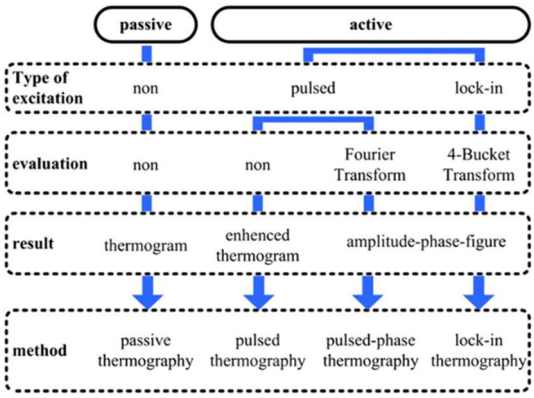

Figure 1– Classification of active thermography methods. Source: An et al (2012).

2.3 STEEL BH220

To meet the requirements of the automotive industry, steel mills have sought to develop high formability and high mechanical strength steels (Ferreira et al, 2012). The search for more resistant materials comes from the need to reduce the weight of vehicles and thus contribute to the reduction of fuel consumption and the emission of pollutants into the atmosphere (Ferreira et al, 2012).

These steels are characterized by being easily formable and by presenting an increase in mechanical resistance due to the phenomenon of aging, which can occur during the heat treatment at low temperature, or in the case of automobile manufacturers, during the curing process of the painting, after the stamping operations.

Cold-rolled steels with controlled aging (bake hardenable - BH) have been widely used by the automotive industry for the production of external car panels (Ferreira et al, 2012). Steel BH220 is an example of this type of steel and has the necessary characteristics to perform well in the automotive industry.

3. METHODOLOGY

3.1 TEST SPECIMEN PREPARATION

For this study, 3 different sizes of specimens of different sizes were defined, as shown in Figure 2, and for each size 5 specimens were built. Specimens 1 and 5, from each Specimen of evidence, were used only for adjustments and tests outside the standard established for the tests. The specimens were manufactured using BH 220 steel sheets with a thickness of 1 mm.

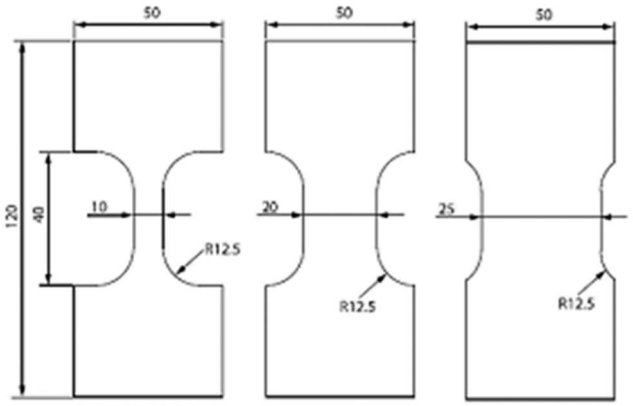

Figure 2 – Specimens - Source: The author – Nakazima test standard edition (2023).

The specimens were classified according to Table 1:

Table 1 – Specimens codes and characteristics. Source: The authors (2023).

Specimen type	Label (small / medium / large)	state	Observation
Thin 1 – 10mm	-	discarded	none
Thin 2 – 10mm	S1	tested	used result
Thin 3 – 10mm	S2	tested	used result
Thin 4 – 10mm	S3	tested	used result
Thin 5 – 10mm	-	discarded	none
Medium 1 – 20mm	-	discarded	none
Medium 2 – 20mm	M1	tested	used result
Medium 3 – 20mm	M2	tested	used result
Medium 4 – 20mm	M3	tested	used result
Medium 5 – 20mm	-	Tested with paint	unused result
Thick 1 – 25mm	-	discarded	none
Thick 2 – 25mm	L1	tested	used result
Thick 3 – 25mm	L2	tested	used result
Thick 4 – 25mm	L3	tested	used result
Thick 5 – 25mm	-	Tested with paint	unused result

3.2 TEST EQUIPMENT

The specimens were subjected to tensile tests using Instron 8801 equipment.

The equipment was adjusted to carry out the tensile test with a constant upper grip velocity with immediate stop after the breakage of the Specimen. The sampling rate of the voltage applied to the specimen is 1ms (One millisecond).

3.3 PREPARATION OF THE TEST ENVIRONMENT

Next to the test equipment, a thermal camera from the brand Flir®, model C2, was installed on a pedestal to capture the temperature in the specimen during the execution of the test. The camera was positioned as perpendicular as possible to the plane of the specimen in order to, when take a photo, obtain the best heat emission from the Specimen. To avoid interference from external thermal radiation, white cloths were arranged in the background, thus minimizing this influence. The assembly of the site can be seen as shown in Figure 4.

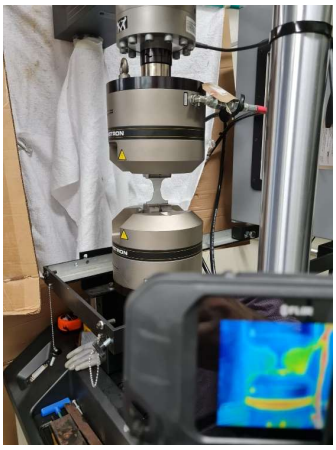

Figure 4 – Test environment. Source: The authors (2023).

The temperature of the room at the time of the tests was obtained through the thermocouple of the thermal cabin of the traction test equipment, which was verified as 25°C (Twenty-Five Degrees Celsius).

3.4 CAMERA PREPARATION

The camera adjustment took into account an emissivity of 0.95 to make the camera's temperature measurement match the reading from a pyrometer that measures the specimen's temperature, so that both readings are the same.

The camera was also adjusted to capture images at an interval of 0.4 seconds (15 frames per second), which is the highest possible speed for this camera model. The camera was used in filming mode to generate the capture of images and after that the processing and generation of data. Table 2 shows the parameters used in the camera adjustment.

Table 2 – Title of specimens. Source: The authors (2023).

Parameters	Value
Emissivity	0.95
Reflective Temperature	40.0ºC
Distance	0.5m
Atmospheric temperature.	25.0 ºC
External. optics temperature.	25.0 ºC
External. optics transmission.	1.0
Relative humidity	50.0%

Due to the fact that the camera and the tensile test equipment do not have an interface that allows the synchronization of events, both the beginning of the test and filming as well as the end of the process were carried out through manual synchronization.

The camera was connected to a notebook which captured the images (videos) as well as the camera settings for the experiment.

3.5 EXECUTION OF TESTS

The tests were performed by applying an axial traction force on the specimens, promoting deformation in the material, stretching the specimen until it fractured.

During this process, the equipment used in the test read the force (in Newtons - N) as well as the elongation of the specimen (in millimeters - mm) at a rate of 10 sample per second. The applied force is dynamic and its increments are based on the characteristics of the material to be tested. These results were saved in a CSV (Character-separated value) file. Figure 5 shows specimen Specimen S1 after fracture and Figure 6 shows specimen Specimen L1 after fracture.

Figure 5 – S1 specimen after completion of the test Source: The authors (2023).

Figure 6 – Specimen L1 after completion of the test Source: The authors (2023).

In conjunction with this test, the thermographic camera was activated at the same time the test started and a standard proprietary file from the camera manufacturer company was generated with the .seq extension. This file is similar to a video, but it brings together the image captures the temperature obtained in each pixel (smallest graphic element of each image). After the image capture was finished, the file was post-processed in the FLIR Tools+® application. This application allows you to extract temperature data frame by frame at a given point, line or area.

The option chosen for data extraction was the line where the result is the maximum, average and minimum temperature in the line. The temperature was read along a line in the longitudinal axis of symmetry of the specimen.

Figure 7 shows a table with the line reference (Li1) and the maximum and minimum temperature indications on the line and its location on it.

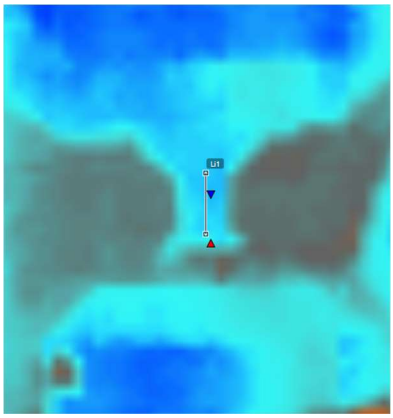

Figure 7 – Screenshot Treatment Image Line LI1 Source: The authors (2023).

Table 3 shows the application values returning to the defined line.

Table 3 – Temperature in LI1 in a frame (2023).

LI1	Value
Max	27.0ºC
Min.	26.8ºC
Average	26.9ºC

In the same way as the force on the specimen, the stress readings were extracted and a CSV file was generated together with the temperature readings of the different frames of the capture. The data used were the reading of the highest temperature in the specimens.

Figure 8 shows the results of force(N) under the various specimens, and it is possible to observe a relative similarity in the data obtained for each set of specimens.

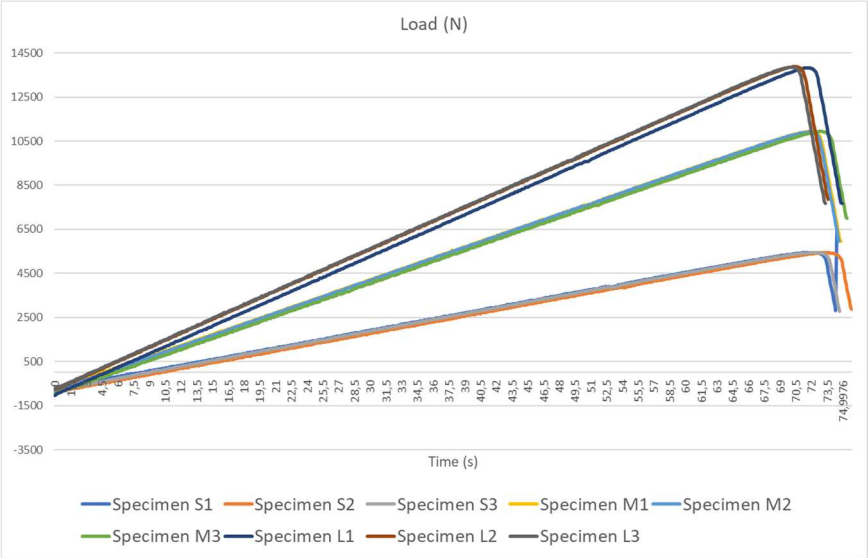

Figure 8 – Data collected Strength. Source: The authors (2023).

Figure 9 shows the results of the temperature in the specimens, obtained through the post-processing of the images obtained by the thermographic camera. In this graph, it is possible to verify a similarity in the data, but with an oscillation during the period of stable temperature and a slightly greater variation during the moments preceding the rupture. There are all cases, in the most stable period the variation did not exceed 2% of the average value.

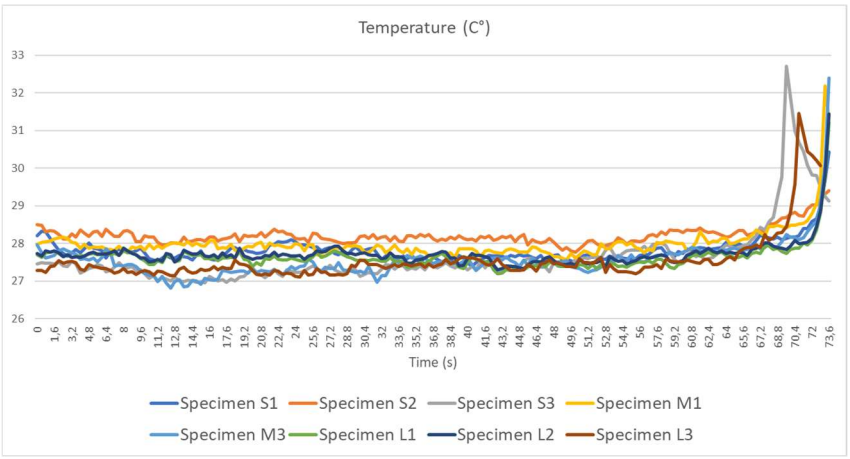

Figure 9 – Data Collected Temperature. Source: The authors (2023).

4. RESULTS PRESENTATION

Figure 10 shows the comparative evolution of stress and temperature in the specimens.

It is possible to observe that, in general, the temperature increases abruptly almost simultaneously with the approach of the breaking point of the specimen. The red lines mark the point of maximum tensile force on the specimen. In Figure 11(c) the large lag between the maximum temperature and when the maximum stress occurs was caused by the miss of synchronism of both measuring process.

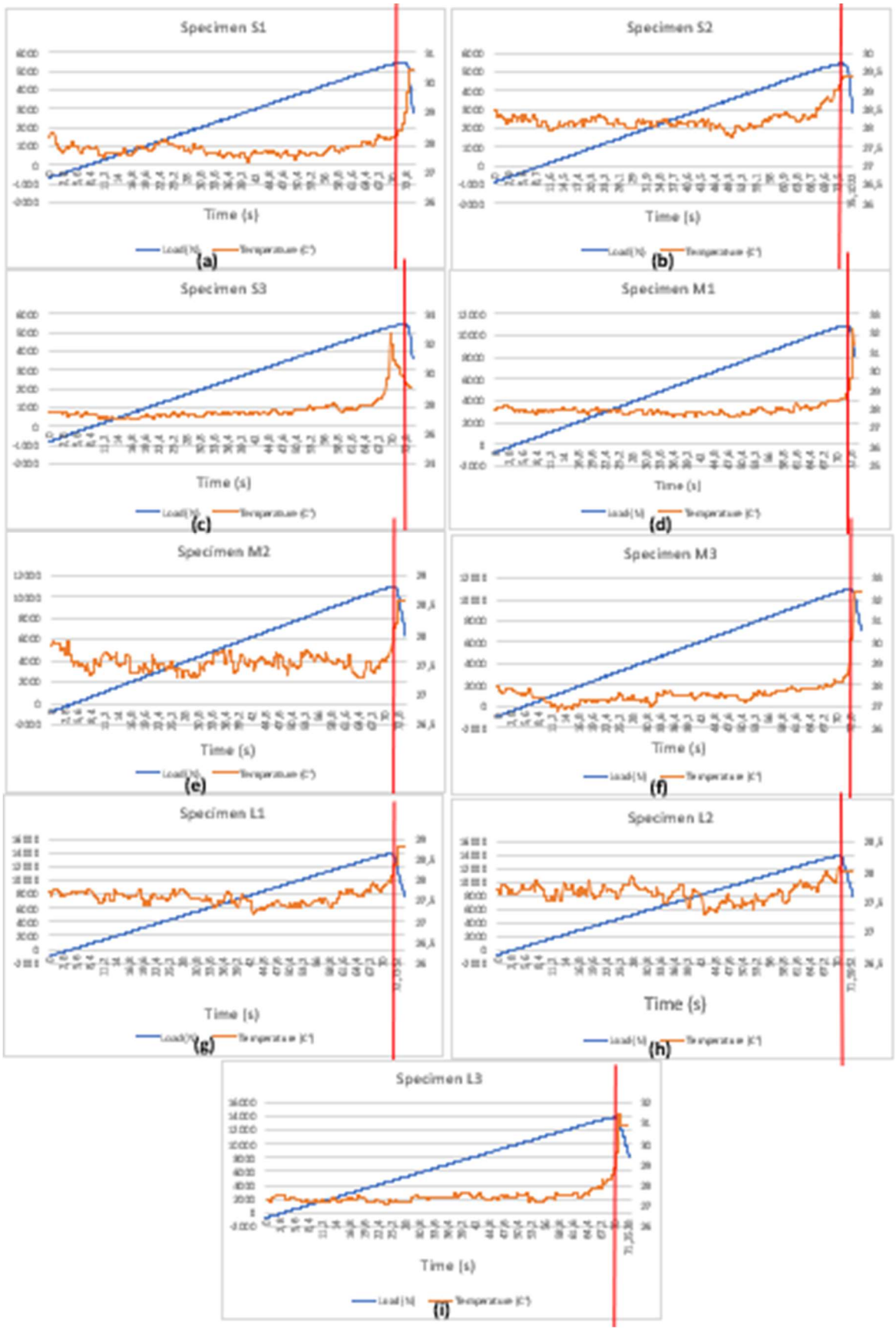

Figure 10 – Comparison of Strength and Temperatures / Time of Specimens. Source: The authors (2023).
(a) Specimen S1;(b) Specimen S2; (c) Specimen S3; (d) Specimen M1; (e) Specimen M2; (f) Specimen M3; (g) Specimen L1; (h) Specimen L2; (i); Specimen L3

Figure 11 shows the result of percentage temperature variation in the various specimens during the tests. It is evident from the graph that, although there are oscillations during the initial phase of the tests, the temperature close to the rupture starts to increase when it exceeds 2% of the average variation and only decreases again after the rupture. The variation was calculated based on the total temperature average to all specimens' measures, relative to temperature at each time of the measurement. So the positive numbers occur when the local point temperature is high then the average and the negative and the temperature was below of the measure.

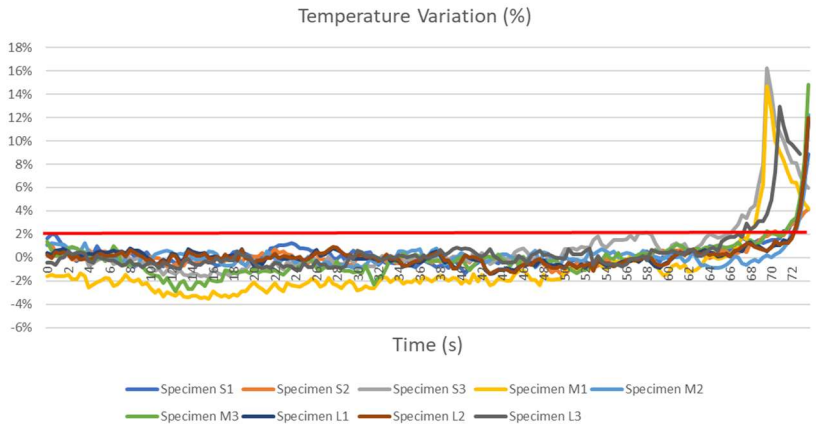

Figure 11 – Global analysis of percentage temperature variation in all specimens. Source: The authors (2023).

Table 4 summarizes the collected data and indicates the maximum points obtained in the tests.

Table 4 – Summary analysis of maximum points. Source: The authors (2023).

Sample	**Data in point of rupture**			**Temperature (C°) during the test**				**Percentage Analysis**	
Specimen	Strength(N)	Temperature (Cº).	Time (s)	Max.	Standard deviation	Average	Time (s) of Max.	Breaking point	Average
S1	5445	28.3	71.7	28.9	0.329	27.7	71.6	102%	
S2	5430	29.3	73.4	31.5	0.240	28.1	74.8	104%	104%
S3	5439	29.8	72.4	32.7	0.824	27.3	70	109%	
M1	10934	28.8	71.9	32.1	0.466	27.9	73.2	103%	
M2	10907	27.7	71.2	31.3	0.347	27.5	73.6	101%	103%
M3	10931	28.4	72.9	32.3	0.515	27.5	73.6	103%	
L1	13817	28.0	71.9	31.2	0.360	27.5	73.6	102%	
L2	13868	28.0	70.6	31.4	0.365	27.6	73.6	101%	102%
L3	13846	28.8	70.1	31.4	0.632	27.3	70.8	105%	

The percentage analysis was calculated based on the total median temperature on each specimen divided by the temperature of the timing measured. The breaking point´s percentage is the value at the time when the temperature starts to increase without reduce again, until the specimen break. The average is the value of the mean temperature to each size of specimens.

It is possible to verify that, in general, the breaking point happens when the temperature exceeds 102% of the average, which indicates that it is possible to correlate the temperature of the specimen with the breaking point. Another analysis that can be done is that, the greater the width of the specimen, the average temperature at the breaking point decreases.

5. FINAL CONSIDERATIONS

The analysis of the results indicates that there is a possible relationship between the temperature of the BH 220 steel, extendable to others steels, and the stress close to the breaking point.

This indicates that it is possible to improve the process and validate an automatic way to detect rupture early and thus avoid it. The use of machine learning using unsupervised methodologies is a possible alternative for automating the prior failure detection process in this case.

As a reference average, rupture occurs after the specimen reaches 102% of the average temperature throughout the test, which makes this value a possible limit temperature reference in the process.

This answers the question, validating that it is possible to use thermographic analysis to predict failures in forming and avoid rupture of BH 220 steel plates by using an automated machine learning process to stop the process or adjust any feasible parameters on the machine. This method needs to be more investigated to define how to implement this on a real machine.

Throughout the experiment, it was possible to verify that the camera used does not have good accuracy to have more accurate data, as well as the setting up of the environment was subject to external interference that, even minimized, may have undergone variations.

We can suggest that in future works the data acquisition process be improved by using a camera with higher definition/resolution range, performing the synchronization between the camera and the test equipment to avoid time variations as well as preparing tests to verify the impact of interferences external in the process since the environment of use of a possible solution does not allow a control so close to that of a laboratory.

6. REFERENCES

A.Erman. Tekkay ,P.-O. Bouchardb, S. Bruschi , C.C. Tasand . 2005 “Damage in metal forming” . CIRP Annals - Manufacturing Technology.

Andrade, SL, Taiss, JM, Rosa, LK , 2002 . “Steel in the car of the future”. In: 57th Congress of the Brazilian Association of Metallurgy and Materials, 2002, São Paulo, Anais... São Paulo, July.

Bhattacharya, Debanshu. , 2014. “Microalloyed Steels for the Automotive Industry”. Technology in Metallurgy, Materials and Mining, p. 371–383.

Francesco. Ancona, R. De Finis, GP Demelio, U. Galietti, D. Palumbo. 2016. Politecnico di Bari, Department of Mechanics, Mathematics and Management, Viale Japigia 182, 70126, Bari, Italy,.

Ferreira, RF et al., 2012” Feasibility study on the use of the BH220 material to replace PEP04 in the external panel of a car”. In: 67th ABM Congress, Anais... Belo Horizonte,.

Ferreira, RF et al., 2013. “Influence of temperature and length of stay in the BH220 steel oven in the result of Bake Hardening” (BH). In: 67th ABM Congress, Anais... Belo Horizonte,.

Luchi, E. ., 2018 “Applications of the infrared thermography in the energy audit of buildings: A review”, Renewable and Sustainable Energy Reviews. v. 82, part 3, p. 3077-3090.

M. Rodríguez-Martina, , S. Laguelaa, B, D. Gonzalez-Aguileraa, J. MartinezbB, 2015– “Prediction of depth model for cracks in steel using infraredthermography” - Infrared Physics & Technologyjournal homepage: www.elsevier.com/locate/infrared .

Q. Ann, D. Horting, M. Merklein , 2012 . “Infrared thermography as a new method for quality control of sheet metal parts in the press shop” - archives of civil and mechanical engineering .

Silva, GP, Batista, PIB, Povóas, YV,2019 "The usage of infrared thermography to study thermal performance of walls: a bibliographic review", Revista ALCONPAT, 9 (2), pp. 117 – 129,

Shun-Peng Zhu a,b,* , Wen-Long Ye a , Jos´e AFO Correia c,d,e , Abílio MP Jesus c , Qingyuan Wang f,g,. 2022. ” Stress gradient effect in metal fatigue: Review and solutions”. - Theoretical and Applied Fracture Mechanics.

Yasser S. Mohameda, Hesham M. Shehataa, Mohamed Abdellatifb, C, Taher H. Awad , 2022. “Steel crack depth estimation based on 2D images using artificial neural networks” - Alexandria Engineering Journal Volume 58,

7. RESPONSIBILITY NOTICE

The author(s) is (are) the only responsible for the printed material included in this paper.